

# Chapter 1

## Friction Force Microscopy

Roland Bennewitz

**Abstract** This chapter introduces Friction Force Microscopy, which is possibly the most important experimental technique in nanotribology. In spite of the apparent simplicity of this technique, a special care is required in the calibration of the force sensors, as discussed in the chapter. We will also present a few key results on the load, material and temperature dependence of friction. The chapter ends with an overview on dynamic measurements of friction, in which the probing tip is oscillated laterally while sliding in contact with the sample surface or even while translating at very close distance from it.

### 1.1 Introduction

Friction Force Microscopy (FFM) is a sub-field of scanning force microscopy addressing the measurement of lateral forces in small sliding contacts. In line with all scanning probe methods, the basic idea is to exploit the local interactions with a very sharp probe for obtaining microscopic information on surfaces in lateral resolution. In FFM, the apex of a sharp tip is brought into contact with a sample surface, and the lateral forces are recorded while tip and sample slide relative to each other. There are several areas of motivation to study FFM. First, the understanding of friction between sliding surfaces in general is a very complex problem due to multiple points of contact between surfaces and the importance of lubricants and third bodies in the sliding process. By reducing one surface to a single asperity, preparing a well-defined structure of the sample surface, and controlling the normal load on the contact the complexity of friction studies is greatly reduced and basic insights into the relevant processes can be obtained. Furthermore, with the decrease of the size of mechanical devices (MEMS) the friction and adhesion of small contacts becomes a technological issue. Finally, the lateral resolution allows to reveal tribological contrasts caused by material differences on heterogenous surfaces.

---

R. Bennewitz (✉)

INM–Leibniz Institute for New Materials, Saarbrücken, Germany  
e-mail: roland.bennewitz@inm-gmbh.de

© Springer International Publishing Switzerland 2015

E. Gnecco and E. Meyer (eds.), *Fundamentals of Friction and Wear on the Nanoscale*,  
NanoScience and Technology, DOI 10.1007/978-3-319-10560-4\_1

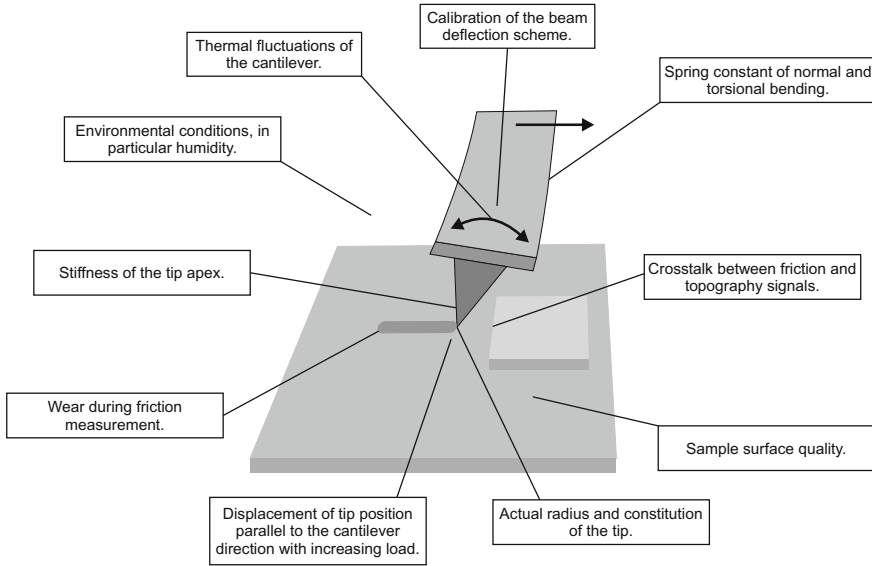


**Fig. 1.1** Critical issues in experimental friction force microscopy which are discussed in this chapter

The experimental field of FFM has been pioneered by Mate et al. [1]. The group built a scanning force microscope where the lateral deflection of a tungsten wire could be measured through optical interferometry. When the etched tip of the tungsten wire slid over a graphite surface, lateral forces exhibited a modulation with the atomic periodicity of the graphite lattice. Furthermore, an essentially linear load dependence of the lateral force could be established.

In this chapter we will describe aspects of instrumentation and measurement procedures. In the course of this description, a series of critical issues in FFM will be discussed which are summarized in Fig. 1.1.

## 1.2 Instrumentation

### 1.2.1 Force Sensors

The force sensor in the original presentation of FFM by Mate et al. was a tungsten wire [1]. Its deflection was detected by an interferometric scheme where the wire constituted one mirror of the interferometer. A similar concept was later implemented by Hirano et al., who optically detected the deflection of the tungsten wire in a Scanning Tunneling Microscope when scanning the tip in close proximity to the surface [2]. Mate and Hirano report lateral spring constants from 1.5 to 2,500 N/m, depending on the wire thickness and length. Etching the wire to form a tip at its end,

mounting the wire, aligning of the light beam, and determination of the spring constant comprise some experimental difficulties. These difficulties are greatly reduced by the use of dedicated micro-fabricated force sensors. A very sophisticated instrumental approach to the solution of those problems has been realized by Dienwiebel et al. [3]. The group has attached a stiff tungsten wire to a micro-fabricated force sensor made of silicon. The central part of the sensor is a pyramid holding the tip. The position of the pyramid is detected in all three dimensions by means of four optical interferometers directed towards the faces of the pyramid. It is suspended in four symmetric high-aspect ratio legs which serve as springs with isotropic spring constant in both lateral directions and a higher spring constant in normal direction. The symmetric design of the instrument allows for determination of normal and lateral forces acting on the tip with minimal cross talk. An overview over different experimental realizations of FFM is given in Fig. 1.2.

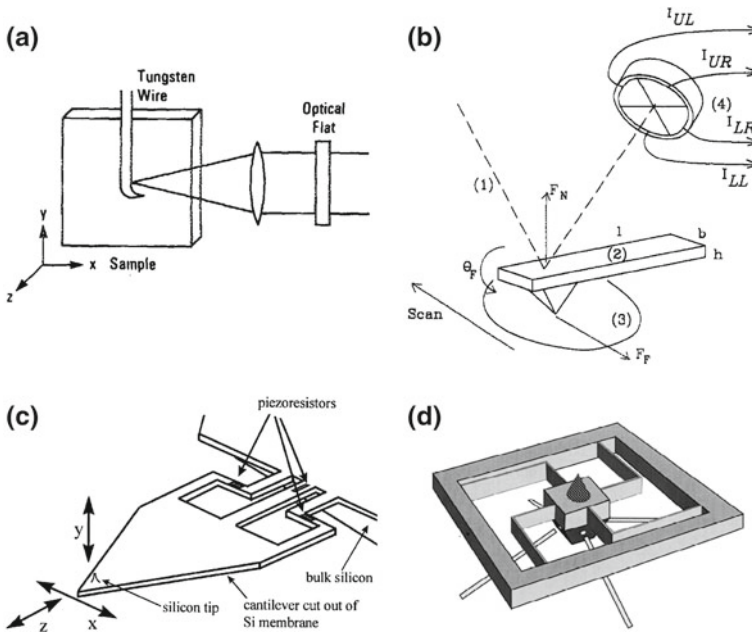


**Fig. 1.2** Four design options for Friction Force Microscopy. **a** Concept of the original instrument used by Mate et al. for their pioneering experiments [1] The deflection of a tungsten wire is detected by optical interferometry. The bent end of the wire is etched into a sharp tip. **b** Beam-deflection scheme as devised by Marti et al. [5]. Normal force  $F_N$  and friction force  $F_F$  cause bending and twisting of the cantilever. The deflection of a reflected light beam is recorded by comparing currents from four sections of a photodiode. **c** Cantilever device for the measurement of lateral forces with piezoresistive detection [8]. Lateral forces acting on the tip cause a difference in stress across the piezoresistors. **d** Micro-fabricated force detector for isotropic measurements of friction forces. The block in the center holds a tungsten tip, pointing upwards in this figure. The position of the block in all three dimensions is recorded by four interferometric distance sensors which are indicated by the four light beams below the devices [9]

The most widely used form of micro-fabricated force sensors for FFM is the micro-fabricated cantilever with integrated tip. The cantilever can be either a rectangular beam or a triangular design based on two beams. The lateral force acting on the tip is detected as torsional deflection of the cantilever. This scheme has been implemented in 1990 by Meyer et al. [4] and Marti et al. [5]. It is interesting to note that the triangular design is more susceptible to deflection by lateral forces than the rectangular beam, contrary to common belief and intuition [6]. However, triangular cantilevers are less prone to the highly unwanted in-plane bending [7].

The deflection of cantilever-type force sensors is usually detected by means of a light beam reflected from the back side of the cantilever at the position of the tip. The reflected light beam is directed towards a position-sensitive photodiode which detects normal and torsional bending of the cantilever as a shift in the position of the light beam in orthogonal directions. Realistically, there is always some cross-talk between the signals for normal and torsional bending. It can be detected by exciting the cantilever to oscillate at the fundamental normal and torsional resonance and measuring the oscillation amplitude in the orthogonal channels. The cross-talk can be minimized by rotation of the position-sensitive photodiode or accounted for in the detection electronics or software. Cross-talk can transfer topographic features into the lateral force signal and create topographic artifacts from friction contrast, the latter even amplified by the feedback circuit acting on the sample height.

Calibration of the beam-deflection scheme is not a simple task, however very important in order to compare FFM results from different sources. Many publications in the past have reported on relative changes in frictional properties, without providing any calibration at all. While such relative changes certainly represent important physical findings, it is nevertheless of utmost importance to provide all experimental information available, often allowing for a rough quantitative estimate of the lateral forces. Lateral forces in FFM can easily range from piconewton to micronewton, spanning a range of very different situations in contact mechanics, and knowing at least the order of magnitude of forces helps to sort the results qualitatively into different regimes.

The calibration comprises two steps. First, the spring constant has to be determined for the force sensor. Note that the beam-deflection scheme actually determines the angular deflection of the cantilever. Nevertheless it has become custom to quantify the force constant in N/m, where the length scale refers to the lateral displacement of the tip apex relative to the unbent cantilever. Second, a relation between the deflection of the cantilever and the voltage readout of the instrument has to be established.

For the determination of the spring constant, several methods have been suggested. The easiest to calculate it from the dimensions of the cantilever. While width and thickness are easily determined by optical or electron microscopy, thickness is better deduced from the cantilever's resonance frequency. Alternatively, the spring constant can be determined from changes in the resonances caused by the addition of masses to the free end of the cantilever. Also, the analysis of a cantilever's resonance structure in air can provide the required quantities. The latter two methods have recently been described and compared by Green et al. [10]. The relation between tip displacement

and voltage readout can be established by trapping the tip in a surface structure and displacing the sample laterally by small distances. For a rough estimate one can also assume that the sensitivity of the position-sensitive photodiode is the same for normal and torsional deflection. Taking into account the geometry of the beam-deflection scheme, the torsional deflection sensitivity can be deduced from the normal deflection sensitivity (See [11] and page 352 of [12]). Since the quantification of the thermal noise driven torsional resonance can be difficult, a combination of thermal noise and beam geometry methods can be useful for the calibration of FFM [13].

A method which provides a direct calibration of the lateral force with respect to the readout voltage is the comparison with a calibrated spring standard. Recent implementations of this approach suggest as calibrated standards optical fibers [14] or micro-fabricated spring-suspended stages with spring constants that can be traced to international standards [15]. Similarly, the lateral stiffness of a magnetically levitated graphite sheet can be used as [16]. A particularly elegant method to calibrate FFM experiments is the analysis of friction loops, i.e. lateral force curves from forward and backward scans, recorded across surfaces with well-defined wedges [11, 17, 18]. Dedicated micro-fabrication design in form of a hammer-shaped cantilever can also help to calibrate the torsional bending [19].

The torsional deflection of a cantilever can in principle be detected also by optical interferometry, provided that the beam diameter is smaller than the cantilever and the point of reflection is shifted off the torsional axis [20]. However, FFM results including normal and lateral force measurements require the differential reading of multiple interferometers [3, 21].

An alternative to the detection of the cantilever bending via the beam-deflection scheme is the implementation of piezoresistive strain sensors into the cantilever. In order to measure both lateral and normal forces acting on the tip in FFM, two such strain sensors need to be realized on one sensor. Chui et al. have created a piezoresistive sensor which decouples the two degrees of freedom by attaching a normal triangular cantilever to a series of vertical ribs sensing lateral forces [22]. Gotszalk et al. have constructed a U-shaped cantilever with one piezoresistive sensor in each arm, allowing for the detection of lateral forces at the tip [23]. While the publications presenting these novel instrumental approaches contain experimental proofs of concept, no further use of piezoresistive sensors in FFM experiments has been reported. This is certainly due to a lack of commercial availability. Furthermore, the signal-to-noise ratio in static force measurements using piezoresistive cantilevers seems not to reach that of optical detection schemes.

### ***1.2.2 Control Over the Contact***

The exact knowledge of the atomic configuration in the contact between tip apex and surface is prerequisite for a complete understanding of the results in Friction Force Microscopy. It is the most severe drawback in FFM that this knowledge is not available in most cases. While sample surfaces can often be prepared with atomic

precision and cleanliness, the atomic constitution of the tip apex is usually less controlled. Friction signals vary with tip shape, as has been investigated for steps on graphite [24]. Furthermore, in the course of sliding atoms may be transferred from the tip to the surface or vice versa. Such transfer processes occur even for very gentle contact formation, as shown in experiments combining Scanning Probe Microscopy with a mass spectrometry analysis of the tip apex [25–27]. The transfer of atoms may quite often not only quantitatively but also qualitatively change the lateral forces encountered. Chemical reactions between surface and tip have been found to significantly increase friction between a Pt(111) surface for silicon but not for diamond tips [28]. The occurrence of atomic stick-slip motion can depend on the establishment of a certain degree of structural commensurability between tip and surface in the course of scanning [29, 30]. For atomic stick-slip measurements on graphite surfaces, the role of small graphite flakes attached to the tip has long been discussed and recently confirmed experimentally [1, 31].

The best control over the atomic structure of the tip apex has been achieved for metal tips in vacuum environments. By applying the established procedures of Field Ion Microscopy (FIM), the tip structure can not only be imaged but also conditioned on the atomic scale. Cross et al. have characterized the adhesion between a tungsten tip and a gold surface and proved the conservation of the atomic tip structure by means of FIM [32]. Even with instruments of lower resolution, FIM can at least be used for cleaning procedures and for a determination of the crystalline orientation of the apex cluster [2].

The integrated tips at the end of micro-fabricated silicon cantilevers have a well-defined crystalline orientation, usually pointing with the (100) direction along the tip. However, the tip surface and with it the whole tip apex are at least oxidized and possibly contaminated through packaging, transport, and handling. Furthermore, many tips are sharpened in a oxidation process which introduces large stresses at the apex. While etching in hydrofluoric acid can remove the oxide and for some time passivate silicon surface bonds by hydrogen, a stable formation and reproducible characterization comparable with FIM of metal tips has not yet been reported. Tips integrated into silicon nitride cantilevers are amorphous due to the chemical vapor deposition process and may exhibit an ever more complex structure and chemistry at the tip apex.

One way of overcoming the uncertainty of the tip constitution is to use methods of surface chemistry to functionalize the tip [33]. Specific interactions between molecules attached to the tip and molecules on the surface can be sensed by means of FFM [34]. At the same time, very strong adhesion has been reduced by covering the tip with a passivating layer to allow for lateral force imaging for example on silicon [35]. Numerous studies using this method have been published, mainly concentrating on organic monolayers on tip and surface. A review of the field has been given by Leggett et al. [36]. While most tip functionalization relies on thiol bonding to gold-coated tips, carbon bonding to nanocrystalline diamond tips has also been realized [37]. Schwarz et al. have prepared well-defined tips for FFM by deposition of carbon from residual gas molecules in a Transmission Electron Microscope, keeping control of the tip radius for a quantitative analysis of a contact mechanics

study [38]. Force measurements explicitly aiming at interactions between colloidal particles and a surface have been performed by gluing micrometer-sized spheres of the desired size to the cantilever [39, 40]. As a final note, one should always be aware of the possible occurrence of major tip wear which has been observed to happen in a concerted action of mechanical and chemical polishing [41].

## 1.3 Measurement Procedures

The standard measurement in FFM is the so-called friction loop: The lateral force acting on the tip is recorded for a certain distance of scanning in the direction perpendicular to the long cantilever axis and for the reverse direction. The area in the loop represents the dissipated energy, and the area divided by twice the distance is the mean lateral force. It is always very instructive to record the topography signal of forward and backward scan at the same time, as differences will reveal cross-talk between normal and torsional bending of the cantilever.

Whenever lateral forces are measured as a function of some experimental parameter, the influence of that parameter on adhesion should be studied simultaneously. In order to interpret the experimental results in terms of contact sizes versus dissipation channels the knowledge of adhesion is essential. An excellent example is the jump in lateral forces observed on a  $C_{60}$  crystal when cooling to the orientational order-disorder phase transition, which was fully explained by a change in adhesion [42]. For experiments carried out in ambient environment, the dominant contribution to adhesion are usually capillary forces which dependent greatly on the humidity and on the hydrophobicity of the surface [43]. The humidity dependence of FFM results itself can depend again on the temperature [44–46]. Consequently, an enclosure of FFM experiments for humidity control greatly enhances the reproducibility of results.

### 1.3.1 *Friction as a Function of Load*

One of the central experiments in tribology is the quantification of friction, i.e. the change of lateral force with increasing normal load on the sliding contact. One of the questions to be addressed is whether the relation between lateral and normal force is linear for FFM experiments, i.e. whether Amontons' law extends to the nanometer scale [47]. The number of FFM studies reporting lateral force as a function of load is very large, and the overall physical picture is multifaceted, to express it in a positive way. A collection of results is shown in Fig. 1.3. From a procedural point of view it is extremely important to measure the lateral forces for the full range of small normal forces until the tip jumps out of contact, usually at a negative normal force. In this way the adhesion in the system can be categorized and even maps of adhesion can be produced from friction versus load experiments [48]. Furthermore,

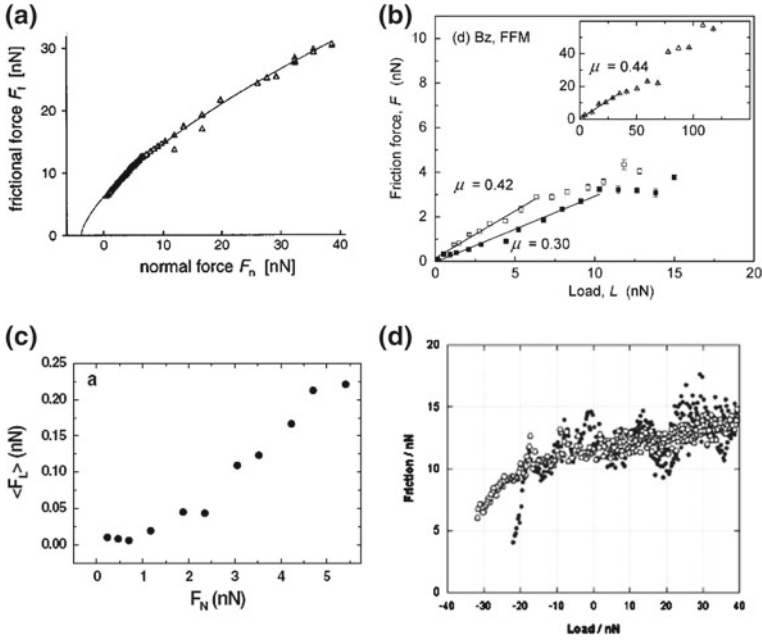


**Fig. 1.3** Examples for the diversity of friction versus load curves measured by FFM. **a** Amorphous carbon measured in an argon atmosphere [38]. The sub-linear characteristic resembles the results of contact mechanics models. **b** Phenyltrichlorosilane monolayer studied in ethanol [50]. A linear dependence is found until the monolayer collapses under the tip pressure. **c** Atomic friction on NaCl(100) recorded in ultra-high vacuum [51]. A regime of vanishing friction is found for low loads. **d** Friction measurement on a hydrogen-terminated diamond surface with nanometer-scale roughness [52]. The closed circles represent the erratic load dependence of FFM results when the lateral displacement of the tip for increasing load is not compensated. The open circles show the expected sub-linear characteristic after activating the compensation

possible nonlinear characteristics at minimal loads are not overlooked. A useful way of analyzing load dependence data from FFM experiments is the representation in lateral force histograms, where for example friction on terraces and friction at steps could automatically be distinguished [49].

When the normal load on the tip is varied the position of the contact may be displaced along the long axis of the cantilever. This effect is caused by the tilt of the cantilever with respect to the surface. On heterogeneous surfaces such displacement may distort the friction measurement and, therefore, has to be compensated [52]. Another effect that can seriously disturb friction experiments is the onset of wear and the concomitant increase of lateral forces. Wear thresholds in FFM can be as low as a few nanonewton normal load, and wear at a constant low load may suddenly start after repeatedly scanning the same area [53].



### ***1.3.2 Friction as a Function of Material***

On inhomogeneous surfaces Friction Force Microscopy can image contrasts between different materials with high lateral resolution. Such contrast has been found to arise from a difference in chemical interactions between different molecular patches at the surface and the tip [54]. FFM can thus serve to identify partial coverage of a surface, for example by graphene patches [55]. As mentioned above, it is crucial to complement lateral friction contrast with local measurements of adhesion in order to elucidate whether adhesion and contact size or different channels of dissipation are dominating the contrast. Care has to be taken regarding topographical artifacts, as different materials on heterogeneous surfaces are often found at different topographic heights. Interestingly, friction contrast is also found between domains of identical molecular layers with anisotropic lateral orientation [56–58]. Friction anisotropy on a given surface has to be clearly distinguished from friction anisotropy for different azimuthal orientations between the tip and the surface. In order to measure the latter, the sample has to be rotated with respect to the tip [31, 59].

### ***1.3.3 Friction Effects in Normal Force Measurements***

When the sample is approached towards the tip, the normal force can be determined as a function of distance by measuring the normal bending of the cantilever. In all beam-deflection type FFM the cantilever is tilted with respect to the sample surface to make sure that the tip is the foremost protrusion of the force sensor. Once the tip is in contact, the tilt causes a lateral displacement of the tip position upon further approach. The friction forces arising from this lateral displacement influence the normal force measurement [40]. A detailed analysis of the process proves that one can actually perform a calibrated friction experiment through normal force versus distance curves, in particular when using extended tips like colloid probes [60]. Even when probing the surface in a dynamic intermittent contact mode these frictional contributions can be detected as a phase shift between excitation and cantilever oscillation [57].

### ***1.3.4 Fluctuations in Friction Force Microscopy***

Friction Force Microscopy is naturally subject to thermal fluctuations. Such thermal fluctuations can influence the frictional behavior of sliding contacts, as evident in the logarithmic dependence of friction on velocity at low scanning velocities [61, 62] which has been linked to thermal fluctuations via its temperature dependence [63]. Cantilever-type force sensors have a distinct resonance structure which dominates the thermal noise spectrum. A full treatment of thermal noise and mechanical vibrations and their influence on FFM have been provided in [64]. Typically, oscillations

at resonances with frequencies of several kHz are averaged out in FFM experiments. However, these resonances influence the experimental result and it is therefore very instructive to study the lateral force signal with high bandwidth [65, 66]. The statistical distribution of lateral forces in atomic stick-slip experiments can be analyzed to reveal the role of thermal fluctuations [67]. The limited scanning velocity of FFM normally separates the frequency regimes of fast fluctuations and of slower occurrence of topographic or even atomic features. The velocity limitations of FFM have been addressed by new designs combining the force sensor of an FFM with a dedicated sample stage [68, 69].

### ***1.3.5 Friction as a Function of Temperature***

The study of friction as a temperature is an obvious field of great interest. However, the number of groups including a temperature dependence into FFM studies is increasing recently [42, 44, 63, 70–74]. Thermal drift is a severe problem in the design of Friction Force Microscopes working at variable temperature, since the optical lever of the beam-deflection scheme needs to have a certain length for sensitivity. Variable-temperature instruments with thermal-expansion compensated design comparable to dedicated Scanning Tunneling Microscopes [75] have not been reported so far. One interesting approach to circumvent drift problems is the local heating of the very tip [46, 76].

### ***1.3.6 Dynamic Lateral Force Measurements***

#### **1.3.6.1 Dynamic Friction Force Microscopy**

When the sample is periodically displaced in lateral direction, the lateral force acting on the tip and detected by the cantilever will be modulated with the same periodicity. An early application of such a lateral modulation by Maivald et al. was the enhancement of contrast at step edges [77]. Dynamic Friction Force Microscopy detects the periodic lateral force signal by means of a lock-in amplifier. This idea was implemented by Göddenhenrich et al., who applied the periodic sample displacement along the long axis of the cantilever and detected the lateral force as periodic buckling of the cantilever [78]. Simultaneously, their fiber-interferometric setup could statically measure the deflection of the cantilever caused by normal forces. The same technique was implemented by Colchero et al. for a beam-deflection instrument. The authors provided a detailed analysis for the evaluation of the lateral forces when the sample is displaced in a sinusoidal movement [79]. They also pointed to the fact that using their method of Dynamic Friction Force Microscopy one will obtain quantitative results when taking data, while static experiments need subtraction of forward and backward scan before numbers can be obtained. Carpick et al. have used a similar

technique with very small sample displacement amplitudes to avoid any slip of the tip over the surface [80]. In such experiments, the amplitude of the lateral force provides a measure for the contact stiffness. Dynamic friction force microscopy has been combined with sophisticated versions of the pulsed-force mode for a simultaneous measurement of all relevant properties of mechanical contacts [81]. In a recently published study, Haugstad has analyzed the non-linear response of the lateral force to the sinusoidal sample displacement in a Fourier analysis [82]. Using this technique he was able to gain new insights into the transition from static to kinetic sliding on a polymer blend.

Dynamic Friction Force Microscopy can gain sensitivity by tuning the periodic excitation to resonances of the cantilever [83, 84]. However, the coupling between the mechanical properties of the contact and the flexural modes of the cantilever require a complex analysis, as provided in a recent review which also references previous work in the field of ultra-sonic force microscopy [85].

### 1.3.6.2 Dynamic Non-contact Lateral Force Experiments

The success of dynamic non-contact force microscopy in atomic resolution imaging of insulating surfaces and its prospect of measuring dissipation phenomena with the same resolution [86] has initiated projects which aim at a dynamic non-contact microscopy using lateral oscillation of the tip. Jarvis et al. have constructed a novel force sensor which allows to excite and detect oscillations of the tip in normal as well as in lateral direction [87]. The independent oscillations were achieved by suspending the tip holder in hinges at the end of two normally oscillating cantilevers. The group has controlled the tip-sample distance by changes in the normal oscillation frequency, and simultaneously recorded changes in the amplitude of the lateral oscillation pointing to frictional tip-sample interactions.

A standard rectangular cantilever has been employed by Pfeiffer et al. for the dynamic detection of interactions between a laterally oscillating tip and a surface close to but not in contact [88]. In this study, the cantilever was excited to oscillate at its first torsional resonance, making the tip oscillate laterally. The distance between tip and a copper surface was controlled using the tunneling current as feedback quantity. The lateral interaction between tip and monatomic steps or single impurities could be detected as frequency shift in the torsional oscillation. Giessibl et al. attached a tungsten tip to a quartz tuning fork such that it would oscillate laterally over the surface. Again using tunneling as feedback, they were able to study dissipation in the lateral movement with atomic resolution on a Si(111)  $7 \times 7$  surface, thereby tracing friction to a single atom [89]. The damping of the lateral oscillation has been explained in terms of a fast stick-slip process involving one adatom. The same surface has recently been studied in dynamic lateral force microscopy using a standard rectangular cantilever by Kawai et al. [90]. In this study a small frequency shift in the torsional resonance frequency upon approach was used to control the tip-sample distance. The torsional resonance was detected using a heterodyne interferometer scheme, where the focus of the light beam was positioned on one side of

the cantilever in order to be sensitive to the torsional bending. This is actually a very informative method to study the resonance structure of cantilevers which can show significant deviations from ideal modeling due to extra masses and asymmetries [20].

The dynamic non-contact experiments introduced in this section are very interesting tools to study conservative and dissipative interactions in lateral motion even before a repulsive contact is established. Their full strength has recently demonstrated by determination of the lateral force needed to move an atom on a surface [91] and by relating atomic structure to the anisotropy of lateral forces [92].

## 1.4 Outlook

Friction Force Microscopy is now a widely distributed experimental method. The experimental procedures and the calibration have been established to allow for reproducible studies of frictional properties in single-asperity contacts. The biggest drawback within the method is the lack of methods for a reproducible preparation and characterization of tips on atomic scale, as compared to the surface preparation by means of methods of Surface Science. Such control over the atomic constitution of the contact area would greatly advance our understanding of tribological processes on the nanometer scale. Other instrumental challenges in the field include the further improvement of FFM experiments at variable temperatures and in liquid environments, where atomic friction phenomena have been observed with a resolution similar to vacuum experiments [93].

## References

1. C. Mate, G. McClelland, R. Erlandsson, S. Chiang, Phys. Rev. Lett. **59**(17), 1942 (1987)
2. M. Hirano, K. Shinjo, R. Kaneko, Y. Murata, Phys. Rev. Lett. **78**(8), 1448 (1997)
3. M. Dienwiebel, E. de Kuyper, L. Crama, J. Frenken, J. Heimberg, D.J. Spaanderman, D. van Loon, T. Zijlstra, E. van der Drift, Rev. Sci. Instr. **76**(4), 43704 (2005)
4. G. Meyer, N. Amer, Appl. Phys. Lett. **57**(20), 2089 (1990)
5. O. Marti, J. Colchero, J. Mlynek, Nanotechnology **1**(2), 141 (1990)
6. J. Sader, R. Sader, Appl. Phys. Lett. **83**(15), 3195 (2003)
7. J. Sader, C. Green, Rev. Sci. Instrum. **75**(4), 878 (2004)
8. T. Gotszalk, P. Grabiec, I. Rangelow, Ultramicroscopy **82**, 39 (2000)
9. T. Zijlstra, J. Heimberg, E. van der Drift, D. van Loon, M. Dienwiebel, L. de Groot, J. Frenken, Sens. Actuators a-Phys. **84**(1–2), 18 (2000)
10. C. Green, H. Lioe, J. Cleveland, R. Proksch, P. Mulvaney, J. Sader, Rev. Sci. Instrum. **75**(6), 1988 (2004)
11. D. Ogletree, R. Carpick, M. Salmeron, Rev. Sci. Instr. **67**(9), 3298 (1996)
12. E. Meyer, R. Overney, K. Dransfeld, T. Gyalog, *Nanoscience: Friction and Rheology on the Nanometer Scale* (World Scientific, Singapore, 1998)
13. R. Alvarez-Asencio, E. Thormann, M.W. Rutland, Rev. Sci. Instr. **84**(9), 096102 (2013)
14. N. Morel, M. Ramonda, P. Tordjeman, Appl. Phys. Lett. **86**(16), 163103 (2005)
15. P. Cumpson, J. Hedley, C. Clifford, J. Vacuum Sci. Technol. B (Microelectron. Nanometer Struct.) **23**(5), 1992 (2005)

16. Q. Li, K. Kim, A. Rydberg, *Rev. Sci. Instr.* **77**(6), 065105 (2006)
17. M. Varenberg, I. Etsion, G. Halperin, *Rev. Sci. Instrum.* **74**(7), 3362 (2003)
18. H. Wang, M.L. Gee, *Ultramicroscopy* **136**, 193 (2014)
19. M.G. Reitsma, R.S. Gates, L.H. Friedman, R.F. Cook, *Rev. Sci. Instr.* **82**(9), 093706 (2011)
20. M. Reinstaedtler, U. Rabe, V. Scherer, J.A. Turner, W. Arnold, *Surf. Sci.* **532–535**, 1152 (2003)
21. G. Germann, S. Cohen, G. Neubauer, G. McClelland, H. Seki, *J. Appl. Phys.* **73**, 163 (1993)
22. B. Chui, T. Kenny, H. Mamin, B. Terris, D. Rugar, *Appl. Phys. Lett.* **72**(11), 1388 (1998)
23. T. Gotszalk, P. Grabiec, I. Rangelow, *Sens. Actuators, A* **123–124**, 370 (2005)
24. Y. Dong, X.Z. Liu, P. Egberts, Z. Ye, R.W. Carpick, A. Martini, *Tribol. Lett.* **50**(1), 49 (2013)
25. U. Weierstall, J. Spence, *Surf. Sci.* **398**, 267 (1998)
26. T. Shimizu, J.T. Kim, H. Tokumoto, *Appl. Phys. A* **66**, S771 (1998)
27. A. Wetzel, A. Socoliuc, E. Meyer, R. Bennewitz, E. Gnecco, C. Gerber, *Rev. Sci. Instrum.* **76**(10), 103701 (2005)
28. A. Caron, D.V. Louzguine-Luzguin, R. Bennewitz, *Acs Appl. Mater. Interfaces* **5**(21), 11341 (2013)
29. A. Livshits, A. Shluger, *Phys. Rev. B* **56**, 12482 (1997)
30. R. Bennewitz, M. Bammerlin, M. Guggisberg, C. Loppacher, A. Baratoff, E. Meyer, H.J. Güntherodt, *Surf. Interface Anal.* **27**, 462 (1999)
31. M. Dienwiebel, G. Verhoeven, N. Pradeep, J. Frenken, J. Heimberg, H. Zandbergen, *Phys. Rev. Lett.* **92**(12), 126101 (2004)
32. G. Cross, A. Schirmeisen, A. Stalder, P. Grütter, M. Tschedy, U. Dürig, *Phys. Rev. Lett.* **80**, 4685 (1998)
33. T. Nakagawa, K. Ogawa, T. Kurumizawa, *J. Vacuum Sci. Technol. B (Microelectron. Nanometer Struct.)* **12**(3), 2215 (1994)
34. C. Frisbie, L. Rozsnyai, A. Noy, M. Wrighton, C. Lieber, *Science* **265**(5181), 2071 (1994)
35. L. Howald, R. Lüthi, E. Meyer, P. Güthner, H.J. Güntherodt, *Z. Phys. B* **93**, 267 (1994)
36. G. Leggett, N.B. NJ, K. Chonga, *Phys. Chem. Chem. Phys.* **7**, 1107 (2005)
37. M.E. Drew, A.R. Konicek, P. Jaroenapibal, R.W. Carpick, Y. Yamakoshi, *J. Mater. Chem.* **22**(25), 12682 (2012)
38. U. Schwarz, O. Zwörner, P. Köster, R. Wiesendanger, *Phys. Rev. B* **56**, 6987 (1997)
39. W. Ducker, T. Senden, R. Pashley, *Nature* **353**, 239 (1991)
40. J. Hoh, A. Engel, *Langmuir* **9**, 3310 (1993)
41. W. Maw, F. Stevens, S. Langford, J. Dickinson, *J. Appl. Phys.* **92**(9), 5103 (2002)
42. Q. Liang, O. Tsui, Y. Xu, H. Li, X. Xiao, *Phys. Rev. Lett.* **90**(14), 146102 (2003)
43. E. Riedo, F. Levy, H. Brune, *Phys. Rev. Lett.* **88**, 185505 (2002)
44. F. Tian, X. Xiao, M. Loy, C. Wang, C. Bai, *Langmuir* **15**(1), 244 (1999)
45. R. Szoszkiewicz, E. Riedo, *Phys. Rev. Lett.* **95**(13), 135502 (23 Sept. 2005)
46. C. Greiner, J.R. Felts, Z. Dai, W.P. King, R.W. Carpick, *ACS NANO* **6**(5), 4305 (2012)
47. J. Gao, W. Luedtke, D. Gourdon, M. Ruths, J. Israelachvili, U. Landman, *J. Phys. Chem. B* **108**(11), 3410 (2004)
48. R. Alvarez-Asencio, J. Pan, E. Thormann, M.W. Rutland, *Tribol. Lett.* **50**(3), 387 (2013)
49. E. Meyer, R. Lüthi, L. Howald, M. Bammerlin, M. Guggisberg, H.J. Güntherodt, *J. Vac. Sci. Technol. B* **14**, 1285 (1996)
50. M. Ruths, N. Alcantar, J. Israelachvili, *J. Phys. Chem. B* **107**(40), 11149 (2003)
51. A. Socoliuc, R. Bennewitz, E. Gnecco, E. Meyer, *Phys. Rev. Lett.* **92**(13), 134301 (2004)
52. R. Cannara, M. Brukman, R. Carpick, *Rev. Sci. Instr.* **76**, 53706 (2005)
53. A. Socoliuc, E. Gnecco, R. Bennewitz, E. Meyer, *Phys. Rev. B (Condens. Matter Mater. Phys.)* **68**(11), 115416 (2003)
54. R. Overney, E. Meyer, J. Frommer, D. Brodbeck, R. Luethi, L. Howald, H.J. Guentherodt, M. Fujihira, H. Takano, Y. Gotoh, *Nature* **359**(6391), 133 (1992)
55. A.J. Marsden, M. Phillips, N.R. Wilson, *Nanotechnology* **24**(25), 255704 (2013)
56. M. Liley, D. Gourdon, D. Stamou, U. Meseth, T. Fischer, C. Lautz, H. Stahlberg, H. Vogel, N. Burnham, C. Duschl, *Science* **280**(5361), 273 (1998)
57. M. Marcus, R. Carpick, D. Sasaki, M. Eriksson, *Phys. Rev. Lett.* **88**(22), 226103 (2002)

58. M. Kwak, H. Shindo, Phys. Chem. Chem. Phys. **6**(1), 129 (2004)
59. H.S. Liao, B.J. Juang, W.C. Chang, W.C. Lai, K.Y. Huang, C.S. Chang, Rev. Sci. Instr. **82**(11), 113710 (2011)
60. J. Stiernstedt, M. Rutland, P. Attard, Rev. Sci. Instrum. **76**(8), 83710 (2005)
61. T. Bouhacina, J. Aime, S. Gauthier, D. Michel, Phys. Rev. B **56**, 7694 (1997)
62. E. Gnecco, R. Bennewitz, T. Gyalog, C. Loppacher, M. Bammerlin, E. Meyer, H. Güntherodt, Phys. Rev. Lett. **84**, 1172 (2000)
63. S. Sills, R. Overney, Phys. Rev. Lett. **91**, 095501 (2003)
64. A. Labuda, M. Lysy, W. Paul, Y. Miyahara, P. Gruetter, R. Bennewitz, M. Sutton, Phys. Rev. E **86**(3), 031104 (2012)
65. T. Kawagishi, A. Kato, Y. Hoshi, H. Kawakatsu, Ultramicroscopy **91**, 37 (2002)
66. S. Maier, Y. Sang, T. Filleter, M. Grant, R. Bennewitz, E. Gnecco, E. Meyer, Phys. Rev. B **72**, 245418 (2005)
67. A. Schirmeisen, L. Jansen, H. Fuchs, Phys. Rev. B **71**, 245403 (2005)
68. N. Tambe, B. Bhushan, Nanotechnology **16**(10), 2309 (2005)
69. E. Tocha, T. Stefanski, H. Schonherr, G. Vancso, Rev. Sci. Instrum. **76**(8), 83704 (2005)
70. X. Yang, S.S. Perry, Langmuir **19**(15), 6135 (2003)
71. R.H. Schmidt, G. Haugstad, W.L. Gladfelter, Langmuir **19**(24), 10390 (2003)
72. L. Jansen, A. Schirmeisen, J.L. Hedrick, M.A. Lantz, A. Knoll, R. Cannara, B. Gotsmann, Phys. Rev. Lett. **102**(23), 236101 (2009)
73. L. Jansen, H. Hoelscher, H. Fuchs, A. Schirmeisen, Phys. Rev. Lett. **104**(25), 256101 (2010)
74. X. Zhao, S.R. Phillpot, W.G. Sawyer, S.B. Sinnott, S.S. Perry, Phys. Rev. Lett. **102**(18), 186102 (2009)
75. M. Hoogeman, D. van Loon, R. Loos, H. Ficke, E. de Haas, J. van der Linden, H. Zeijlemaker, L. Kuipers, M. Chang, M. Klik, J. Frenken, Rev. Sci. Instrum. **69**(5), 2072 (1998)
76. B. Gotsmann, U. Durig, Langmuir **20**(4), 1495 (2004)
77. P. Maivald, H. Butt, S. Gould, C. Prater, B. Drake, J. Gurley, P. Hansma, Nanotechnology **2**, 103 (1991)
78. T. Göddenhenrich, S. Müller, C. Heiden, Rev. Sci. Instr. **65**, 2870 (1994)
79. J. Colchero, M. Luna, A. Baro, Appl. Phys. Lett. **68**, 2896 (1996)
80. R. Carpick, D. Ogletree, M. Salmeron, Appl. Phys. Lett. **70**, 1548 (1997)
81. H.U. Krottil, T. Stifter, O. Marti, Appl. Phys. Lett. **77**(23), 3857 (2000)
82. G. Haugstad, Tribol. Lett. **19**(1), 49 (2005)
83. M. Reinstadtler, U. Rabe, V. Scherer, U. Hartmann, A. Goldade, B. Bhushan, W. Arnold, Appl. Phys. Lett. **82**(16), 2604 (2003)
84. L. Huang, C. Su, Ultramicroscopy **100**(3–4), 277 (2004)
85. M. Reinstadtler, T. Kasai, U. Rabe, B. Bhushan, W. Arnold, J. Phys. D: Appl. Phys. **38**(18), 269 (2005)
86. S. Morita, R. Wiesendanger, E. Meyer, *Noncontact Atomic Force Microscopy*, NanoScience And Technology (Springer, Berlin, 2002)
87. S. Jarvis, H. Yamada, K. Kobayashi, A. Toda, H. Tokumoto, Appl. Surf. Sci. **157**, 314 (2000)
88. O. Pfeiffer, R. Bennewitz, A. Baratoff, E. Meyer, P. Gruetter, Phys. Rev. B **65**, 161403 (2002)
89. F. Giessibl, M. Herz, J. Mannhart, Proc. Natl. Acad. Sci. USA **99**(19), 12006 (2002)
90. S. Kawai, S.I. Kitamura, D. Kobayashi, H. Kawakatsu, Appl. Phys. Lett. **87**(19), 173105 (2005)
91. M. Ternes, C.P. Lutz, C.F. Hirjibehedin, F.J. Giessibl, A.J. Heinrich, Science **319**(5866), 1066 (2008)
92. A.J. Weymouth, D. Meuer, P. Mutombo, T. Wutscher, M. Ondracek, P. Jelinek, F.J. Giessibl, Phys. Rev. Lett. **111**(12), 126103 (2013)
93. A. Labuda, W. Paul, B. Pietrobon, R.B. Lennox, P.H. Gruetter, R. Bennewitz, Rev. Sci. Instr. **81**(8), 083701 (2010)

Fundamentals of Friction and Wear on the Nanoscale

Gnecco, E.; Meyer, E. (Eds.)

2015, XXII, 704 p. 360 illus., 37 illus. in color., Hardcover

ISBN: 978-3-319-10559-8